MEASUREMENT SCIENCE REVIEW, **19**, (2019), No. 1, 35-42

sciendo

ISSN 1335-8871

MEASUREMENT SCIENCE REVIEW

Journal homepage: https://content.sciendo.com

Optimization Paradigm in the Signal Recovery after Compressive Sensing

Linus Michaeli, Ján Šaliga, Pavol Dolinský, Imrich Andráš

Technical University of Košice, Faculty of electrical engineering and informatics,
linus.michaeli@tuke.sk, jan.saliga@tuke.sk, pavol.dolinsky@tuke.sk, imrich.andras@tuke.sk

Compressive sensing is a processing approach aiming to reduce the data stream from the observed object with the inherent sparsity using the optimal signal models. The compression of the sparse input signal in time or in the transform domain is performed in the transmitter by the Analog to Information Converter (AIC). The recovery of the compressed signal using optimization based on the differential evolution algorithm is presented in the article as an alternative to the faster pseudoinverse algorithm. Pseudoinverse algorithm results in an unambiguous solution associated with lower compression efficiency. The selection of the mathematically appropriate signal model affects significantly the compression efficiency. On the other hand, the signal model influences the complexity of the algorithm in the receiving block. The suitability of both recovery methods is studied on examples of the signal compression from the passive infrared (PIR) motion sensors or the ECG bioelectric signals.

Keywords: Compressed sensing, Analog to Information Converter.

1. INTRODUCTION

The main idea of the compressive sensing (CS) is to recover signals using fewer measurements than the number prescribed by the Nyquist theorem for certain classes of signals. In particular, CS allows the reconstruction of the information parameters describing the observed process by a suitable set of basis functions. This recovery is optimal for the signals with low information rate. Low information rate is reflected by sparsity of the signal in the time domain or sparsity in some transformed domain. Reconstruction quality depends on particular reconstruction algorithm being used. Signals describing aperiodic events in monitoring objects can be stored or transmitted in the compressed form. Here can be considered signals from the seismic sensors, movement detectors in the monitored space or the bioelectric signal receiver, etc. The signal in time or transformed domain contains a lot of components with low importance to the signal characterization. Those components can be considered as information samples with zero value, impacted just by superimposed noise or uncertainty error.

There are various architectures aiming to compress signal by AIC at the transmitter based on the wide scale of processing algorithms [1], [2], [3], [13]. The basic structure consists of the cascade of ADC at the input followed by digital modulator where the output data from ADC are multiplied by Pseudo-Random Binary Sequence (PRBS), which provides encryption of sparse input signal. Digital low pass (LP) filter compresses the processed signal by averaging. Signal reconstruction is based on demodulation by the identical PRBS as was used in the compressing phase, and the successive signal estimation by optimization of the recovered signal (Fig.1.) [4], [5], [6]. It is obvious that the algorithm implemented in each CS branch requires an adequate processing procedure in the receiving block. The mathematical constraints and rules in one branch of the parallel AIC are the same as for a parallel structure [7].

This paper is organized as follows. Signal prerequisites for the application of compressed sensing and corresponding signal models in one band are defined in section 2. The contribution of this article is presented in section 3. Here the two basic recovery algorithms are described together with the corresponding AIC architectures. The signal recovery and corresponding compression efficiency are shown on examples of the selected signals in section 4. Finally, section 5 concludes the paper.

2. INPUT SIGNAL SUITABLE FOR COMPRESSED SENSING

Let us consider the signal to be compressed as sparse in time or in the transformed domain. Let us suppose, that it can be described with adequate accuracy by L basis functions, where each one is determined by two parameters a_l, b_l, and the time sample number i [8], [9]. The input signal $f(i)$ carrying the substantial information, sampled according to the Nyquist theorem, is:

DOI: 10.2478/msr-2019-0006

$$f(i)=\sum_{l=1}^{L} x_l \psi_l(a_l,b_l,i), i=1,...,I; \text{ in matrix form}$$
$$\mathbf{f}=\mathbf{\Psi(a,b).x} \tag{1}$$

The dimension of the signal vector **f** is (I×1). The amplitudes x_l of basis functions are included in the vector $\mathbf{x} = [x_1,x_2,\ldots,x_L]^T$. The number of samples I in one processing time frame T acquired with sampling frequency f_s determined for signal spectrum width is $I = f_s T$.

Matrix $\mathbf{\Psi}$ with the dimension (I×L) represents the parametric signal model described by a set of basis functions $\Psi_l(a_l,b_l,i)$.

$$\mathbf{\Psi}=\begin{bmatrix} \psi_1(a_1,b_1,1), & \psi_2(a_2,b_2,1), & \cdots & \psi_L(a_L,b_L,1) \\ \psi_1(a_1,b_1,2), & \psi_2(a_2,b_2,2), & \cdots & \psi_L(a_L,b_L,2) \\ \vdots & \vdots & \ddots & \vdots \\ \psi_1(a_1,b_1,I), & \psi_2(a_2,b_2,I), & \cdots & \psi_L(a_L,b_L,I) \end{bmatrix} \tag{2}$$

In the case of harmonic functions, the parameters a_l, b_l determine frequency and phase. The data stream compression is more efficient for signals which are descriptive by some transform components like wavelet, Daubechies, Walsh-Hadamard, etc.

The simpler signal model $\mathbf{\Psi}$ consists of L non-parametric basis functions $\Psi_l(i)$ of the sample number i. The utilized basis functions may differ in the analytical expression (3).

$$\mathbf{\Psi}=\begin{bmatrix} \psi_1(1), & \psi_2(1), & \cdots & \psi_L(1) \\ \psi_1(2), & \psi_2(2), & \cdots & \psi_L(2) \\ \vdots & \vdots & \ddots & \vdots \\ \psi_1(I), & \psi_2(I), & \cdots & \psi_L(I) \end{bmatrix} \tag{3}$$

In general, any signal can be modeled by a set of L Heaviside functions $\Psi_l(i)$=h(i-l-1) with the specific delays l.

In order to suppress incoherency between processed signal and the model (3), the synchronization signal is required. It determines the point linked with the time frame T. Let us consider constant length of the time frame T for one processing frame marked by a synchronization event. The synchronization signal ensures coherency and suppresses possible leakage effects among signal components $\Psi_l(i)$. Threshold crossing in compressing of the one-shot events like seismic, or an aperiodic process is a typical case, where it is difficult to choose a suitable signal transformation for the data compression.

Contrary to the parametric signal model (2), the non-parametric signal model (3) contains basis functions with exactly defined position and shape in the time frame. The basis functions are not mutually limited by any analytically defined condition. The contribution of each basis function $\Psi_l(i)$ to the signal **f** to be compressed is determined by the vector **x**.

In general, the number of unknown parameters carrying the measurement information represents the sparsity s of the signal. In the case of the signal model (3) the sparsity $s = \beta$, while $s = 3\beta$ in the model (2). Result of the compressed sensing is the reduction of the data stream from I samples down to at least s samples, where $s < I$. Another consideration for further analysis is that one CS procedure is implemented in one processing time frame T. Information parameters **a, b, x** are compressed in the transmitting and recovered in the receiving block for each time frame T. Maximal frequency of the parameter **a, b, x** changes must be lower than the half of processing frame frequency $(T/2)^{-1}$ according to the Nyquist theorem.

The signal acquired from the observed process is corrupted at the input of Analog to Digital Converter (ADC) by additive thermal and quantization noise n_i. Basic consequence of the sparsity in time domain for signal $f(i)$ is the presence of (I-s) samples in the time frame T with zero value or value under uncertainty level.

3. MATHEMATICAL CONCEPT OF COMPRESSED SENSING

The signal sparsity means that a huge amount of samples in the time or in the Fourier domain is without information content. Compressed sensing represents stressing the frequency bandwidth of the transmitted signal. Modulation by wide band random signal breaks the signal coherence and spreads the information content over the whole frequency range. It is achieved by the multiplication of the input signal vector **f** by the measurement matrix $\mathbf{\Phi}$ represented by a set of functions $\boldsymbol{\varphi}_m(i)$, i = 1,...I, formed by the random numbers. They are formed by Gaussian, Pseudo-random or any distribution spreading the spectrum of the signal **f**. Functions $\boldsymbol{\varphi}_m(i)$ are ordered in M mutually uncorrelated rows. Dimension of the measurement matrix $\mathbf{\Phi}$ is (M×I). The multiplication by the measurement matrix $\mathbf{\Phi}$ in one row represents the low pass (LP) filtering and the compression of the data flux. The compressed output signal **y** is equal to

$$\mathbf{y}=\mathbf{\Phi f}=\mathbf{\Phi\Psi x}=\mathbf{Ax}; \quad \text{where} \quad \mathbf{A}=\mathbf{\Phi\Psi} \tag{4}$$

Pseudo-random number generator converges to the uniform distribution with increasing sequence length. Pseudo-Random Binary Sequence (PRBS) is a subgroup of pseudo-random number generator and is represented by the numbers ±1 and can be reconstructed in the receiving block for known length and initial seed value [16], [17].

Let us consider the signal $f(i)$ transformable on the base of signal model $\mathbf{\Psi}$. Signal can be reconstructed according to the measurement matrix $\mathbf{\Phi}$, which is incoherent with the matrix $\mathbf{\Psi}$. The maximum similarity that can be found between basis functions $\boldsymbol{\psi}_l$ and component of the measurement matrix $\boldsymbol{\varphi}_m$ is determined by the mutual base coherence,

$$\mu(\mathbf{\Phi},\mathbf{\Psi})=\sqrt{I}\max_{1\le m\le M,\,1\le l\le L}\left|\boldsymbol{\varphi}_m \bullet \boldsymbol{\psi}_l\right| \tag{5}$$

absolute value represents the product of two vectors. Considering the normalizing factor, the mutual coherence lies in the range of [1, $\sqrt{I}$], and determines the independence between the measuring base and signal base [5], [10]. The minimum required number of compressed samples is

$$M \geq \mu^2(\mathbf{\Phi},\mathbf{\Psi}) s \log I = \left|\text{ideal case } \mu = 1\right| = s \log I \tag{6}$$

The hardware implementation of AIC with the minimal signal processing operation in the analog domain [6], [12] has been chosen. It consists of baseline high-speed ADC with integrated S&H block at the input with ideal code bin width Q and sampling period T_S. Successively, digital signal processing (DSP) is performed in any digital processing unit like FPGA. Digital samples from the ADC output are acquired in one-time frame T and registered in vector **f**. The spectrum spreading is realized digitally in AIC by multiplication by chipping block $p_m(i)$ = (-1 or 1). It is implemented by changing sign according to the output from a subprogram representing PRBS [14]. Requirement on the incoherency between matrices $\mathbf{\Phi}$ and $\mathbf{\Psi}$ is achieved by taking subsequently successive M chipping blocks $p_m(i)$ with the length I from the whole PRBS with the length MI. According to equation (4) the registered input samples modulated by PRBS are summed $y(m) = \Sigma f(i) p_m(i)$ for each chipping block $m = 1,...,M$. The components $y(m)$ defined this way are results of digital low pass (LP) filtering [15], [16]. Compressed digital data stream $\boldsymbol{y}$ of M samples is transmitted to the receiving block. The transmission frequency is M/T, which is lower than input sampling frequency $T_s^{-1} = I/T$.

Compressed digital signal $\boldsymbol{y}$ from AIC is transmitted to the receiver with the frequency rate M/T. The synchronization mark at the beginning of each time frame with M samples is required for recovery of the identical PRBS in the transmitting block.

In the receiving block the signal recovery requires restoration of the matrix $\mathbf{\Phi}$ represented by M rows with the length I created by identical PRBS as it was used in the transmitting block. It can be done on the base of known code length MI and initial value seed of numerically reconstructed PRBS [11], [14]. Both information serve as encoding key for the CS procedure. Identified header synchronization mark is another condition for the recovery of sparse signal **f** parameters from the digital data stream **y** for each data frame.

The receiving block is expected to be implemented on the processing server able to perform the complex mathematical operations sufficiently fast [20], [25]. Structure for the input signal compression and its reconstruction by the recovery of its sparse parameters is shown in Fig.1.

It is based on the minimization of the objective function for l_p norm where p is equal to 1 or 2 over the solution space.

$$\min_{\hat{\mathbf{a}},\hat{\mathbf{b}},\hat{\mathbf{x}}} \left\| \mathbf{y}_{in} - \mathbf{\Phi\Psi}(\hat{\mathbf{a}},\hat{\mathbf{b}})\hat{\mathbf{x}} \right\|_{l_p} \leq \varepsilon \tag{7}$$

Using l_1 norm leads to the minimization by some, i.e. Basis Pursuit, Orthogonal Matching Pursuit, etc. strategies by solving simple convex optimization problems through linear programming [16], [17].

Classical Least Mean Squared (LMS) minimization of l_2 norm represents the universal reconstruction algorithms in CS. It leads to calculation of vector $\hat{\mathbf{x}}$ using pseudoinverse solution of the equation (4). Moreover, the LMS minimization of (7) by suitable optimization algorithm is only a method to reconstruct concurrently two vectors of model parameters $\hat{\mathbf{a}},\hat{\mathbf{b}}$ and weighting vector $\hat{\mathbf{x}}$ for the parametric signal model (2). l_2 norm is more efficient for the recovery of strongly sparse signals in contrary to the l_1 norm. ADC at input causes that noise input samples under ideal code bin width Q will be rounded off to the 0 value. Suppression of thermal noise from analog input increases the sparsity of the compressed signal in DSP.

Let us consider a special case when the matrix $\boldsymbol{A}=\boldsymbol{\Phi\Psi}$ is constant. The non-parametric (3) signal model $\boldsymbol{\Psi}$ meets this condition. If the matrix is a full rank matrix (i.e. $\mathbf{A}^T\mathbf{A}$ exists), then the amplitude vector $\hat{\mathbf{x}}$ is determined by:

$$\hat{\mathbf{x}} = \left(\mathbf{A}^{\mathrm{T}}\mathbf{A}\right)^{-1}\mathbf{A}^{\mathrm{T}}\mathbf{y}_{in} \tag{8}$$

Direct estimation of $\hat{\mathbf{x}}$ using pseudoinverse solution is limited by the condition that the matrix **A** has to have more than M linearly independent rows. This condition is fulfilled thanks to uncorrelated rows in matrix $\mathbf{\Phi}$ generated from the whole PRBS and the full rank signal matrix $\mathbf{\Psi}$.

The reconstruction of the signal described by the parametric signal model (2) excludes the possibility of using analytical calculation of vectors $\hat{\mathbf{a}},\hat{\mathbf{b}},\hat{\mathbf{x}}$. The LMS minimization ($l_2$ norm) of the difference between the target value $\mathbf{y}_{in}$ and its estimation $\mathbf{\Phi\Psi}(\hat{\mathbf{a}},\hat{\mathbf{b}})\hat{\mathbf{x}}$ leads to the nonlinear estimation problem. Vectors $\hat{\mathbf{a}},\hat{\mathbf{b}},\hat{\mathbf{x}}$ contain all s unknown parameters of the sparse signal $f(i)$.

There are many optimization algorithms to estimate all s parameters included in $\hat{\mathbf{a}},\hat{\mathbf{b}},\hat{\mathbf{x}}$. The changes of signal parameters $\mathbf{\Psi}(\hat{\mathbf{a}},\hat{\mathbf{b}})$ after each iteration step represent the drawback of the classical optimization method like gradient descent or quasi-Newton methods which is the possibility of the convergence into the local minima.

The estimation ambiguity caused by the local minima increases with increasing number s of parameters to be estimated.

The metaheuristic optimization based on the differential evolution (DE) strategy restricts this drawback. It optimizes iteratively a candidate solution with regard to a given objective function (7). However, DE optimization does not guarantee that optimal solution is suitable in the case when the objective function is not differentiable corrupted by noise and even not continuous [18], [19]. DE optimizes a population of candidate solutions and creates new candidate solutions by combining existing ones according to its simple formulae. The DE optimization may be accelerated by suitably set parameter boundaries **[x,a,b]** by known signal limits.

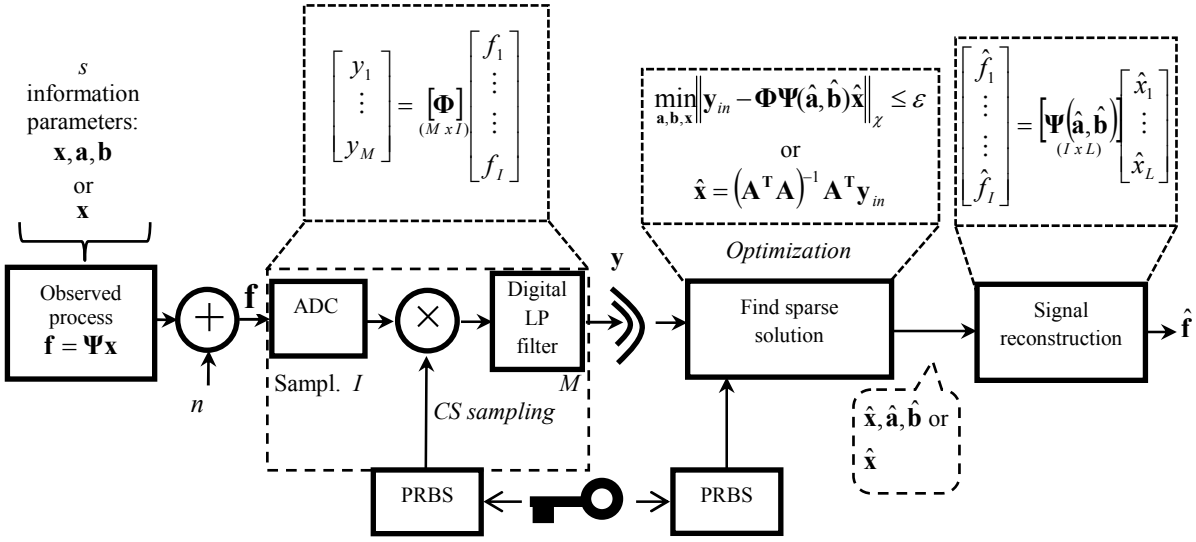

Fig.1. Compressed sensing and recovery.

Theoretical and practical aspects of implemented DE are well prepared for large scale of practical problems without the need for high computing capacity and processing time and suppress the main disadvantage of nonlinear optimization procedure.

The reduction of the data stream from the input to the output of the transmitting block is defined as the compression ratio (CR). Taking into account that just M samples are required for the signal reconstruction in one frame, CR is equal to

$$CR = \frac{I}{M} \tag{9}$$

Accuracy of the recovery paradigm was assessed by the standard deviation between input and recovered signal expressed in dB.

$$\delta_{\mathrm{dB}} = 20\log\left(\frac{1}{f_{RMS}}\sqrt{\frac{\sum_{i=1}^{I}\left(f(i)-\hat{f}(i)\right)^2}{I}}+1\right)\left[\mathrm{dB}\right] \tag{10}$$

Criterion for determining compression accuracy (10) corresponds to the uncertainty type A of DSP unit related to the input signal noise expressed in [dB]. ADC at the input of transmitting block was considered 12-bit linear ADC with peak-peak value $U_{\mathrm{pp}} = 3\mathrm{V}$. The signal noise $f_{RMS} = \sqrt{Q^2/12 + u_{RMS}^2}$ covers ideal quantization noise of ideally linear ADC $u_Q = Q/\sqrt{12}$ and thermal noise u_{RMS} from the analog processing unit at the input. Advancements in ADC make it possible to assume that the dominant uncertainty source is superimposed noise at the AIC input. It is mainly caused by noise from the signal source with superimposed noise from the analog preprocessing unit. Verified compression accuracy includes all potential error sources of its implementation on any DSP unit. A complete estimation of systematic errors requires knowledge of systematic errors of the signal source in the particular case together with the nonlinearity of the actual preprocessing block with integral nonlinearity of ADC at the AIC input. Practical implementations of AIC studied further consider contribution of the signal source nonlinearity under the level of the uncertainty type A.

The first implementation is utilized for the monitoring of moving persons in a defined area. Scope of Ambient Assisted Living is to recognize an emergency situation of the monitored person caused by falling for various reasons. The network of passive infrared (pyroelectric) PIR motion sensors generates signals carrying information for distant server about changes of thermal field caused by movement of the monitored person. The output signal from the PIR sensor is in the form of a flicker with positive and negative part caused by the movement of the monitored persons. Its peak value depends on the distance from any sensor and time interval in zero crossing determines speed of the persons. Time duration of the signal tail is arbitrary and depends on the time intervals of the consecutive movements. Output signal is aperiodic, where the synchronization signal is generated by threshold comparator [22].

Second application suitable for signal compression and successive recording for further evaluation is electrocardiographic (ECG) signal. Even here short delay caused by processing in AIC is harmless and synchronization instant can be taken from the signal of another ECG lead [2], [20], [21].

Short time delay of the information transmission is not deficient. This is balanced by the data compression with adequate accuracy.

4. EXPERIMENTAL RESULTS

Functionality of the AIC utilizing both types of signal models, (2) resp. (3), was assessed experimentally for two applications mentioned above. Time delay for the signal recovery at the end of time frame T is not a disadvantage. Accuracy of the recovery paradigm was assessed according to the criterion (10) in relation to the compression ratio CR (9).

First process where the CS allows compressing basic information is represented by data acquired from the PIR sensor. Fig.2. shows standard output from the PIR sensor BS036B after its preprocessing by the input amplifier [22]. The noise floor caused by EMI and thermal effects influences the input signal at the AIC.

The impulse shape carries the information that has to be transmitted and detected by AIC. In general, such signal could be modeled by the weighted sum of Heaviside functions:

$$\begin{bmatrix} f(1) \\ f(2) \\ \vdots \\ f(I) \end{bmatrix} = \begin{bmatrix} h(0) & h(-1) & \cdots & h(1-L) \\ h(1) & h(0) & \cdots & h(2-L) \\ \vdots & \vdots & \ddots & \vdots \\ h(I-1) & h(I-2) & \cdots & h(I-L) \end{bmatrix} \begin{bmatrix} x(1) \\ x(2) \\ \vdots \\ x(L) \end{bmatrix};$$

$$\text{where} \quad h(j) = \begin{cases} = 0; & \text{for} \quad j \langle 0 \\ = 1; & \text{for} \quad j \geq 0 \end{cases} \tag{11}$$

The initial pulse signal is created by L Heaviside components and other (I-L) samples are negligible and do not carry any information. The trail of the input signal is lower than noise level in this case.

Results from recovery using pseudoinverse algorithm (8) for two length W of averaging LP filter are shown in Fig.3.

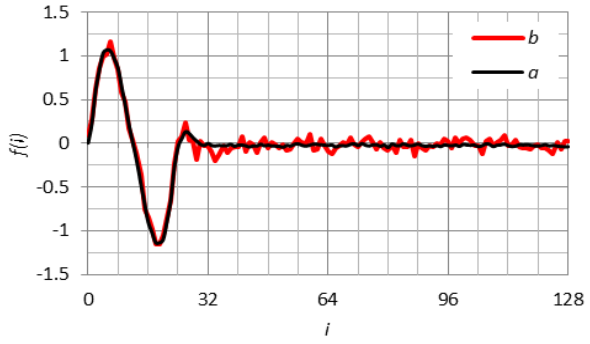

Fig.2. Signal at the input of AIC from PIR sensor with superimposed noise with u_{RMS}=10 mV a) and u_{RMS}=60 mV b). Resolution of input ADC 12 bits, U_{pp}=3 V. Length of recorded signal is 128 samples where 96 are sparse.

Output signals in Fig.3. show that besides the high compression ratio the AIC also acts as a filter removing additive noise at the input AIC. Increasing length W of the LP filter deteriorates time information (Fig.3.b)) and determines CR directly.

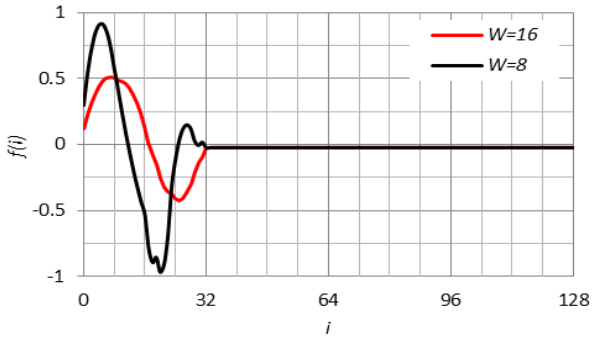

Fig.3. Reconstructed signal from AIC from PIR sensor Fig.2. superimposed noise u_{RMS}=60 mV with LP length W=8 samples a) and W=16 samples b).

The compression ratio of the signal in Fig.3.a) is $CR = 8$ and $\delta_{dB} = 4.56$ dB. In the case of signal from Fig.3.b) is $CR = 16$, but the signal recovery is worse $\delta_{dB} = 29$ dB.

Second case suitable for implementation of CS with parametric signal model (2) was the compression of ECG signal. The optimal selection of basis functions adapted to the observed process allows more effective compression of the observed process. The nonlinear signal model with internal parameters **a,b** of the appropriate basis functions with their peak values **x** achieves better CR. The nonlinear optimization of (7) for $p = 2$ by the DE optimization allows to suppress a false solution represented by local minima.

As signal to be compressed, the electrocardiographic signal was chosen [23], [24]. Basis functions in the form of Mexican hat wavelet $\psi(i) = \left[1 - (i-a_l)^2 / b_l^2\right] \mathrm{e}^{\frac{(i-a_l)^2}{2b_l^2}}$ have been used for its modeling. The optimization behaviors were assessed by simulation for the observed signal in Fig.4. realized by three known wavelets in the form of Mexican hat. The recovery procedure was assessed for various numbers of basis functions starting with the first one. Expected intervals of the initial population were chosen identically for parameters a_l and b_l in the interval between zero and expected maximal value. Initial amplitudes x_l of single components were chosen in the interval ($-U_{PP}$,$+U_{PP}$). Recovered signals for various numbers of basis functions $L = 2,3,4$ in matrix $\boldsymbol{\Psi}$ when input signal is represented by parameters in Table 1. are shown in Fig.5.a) to Fig.5.c).

Table 1. Parameters of modeled input function.

l	a_l	b_l	x_l
1	120	60	2
2	30	120	0.3
3	60	15	0.2
4	0.1	0.01	-0.05

Fig.5. shows that besides improving quality of recovery the noise suppression is inherent behavior of the compressed sensing. Improvement of the signal recovery for various compression ratios CR is shown in Fig.6.

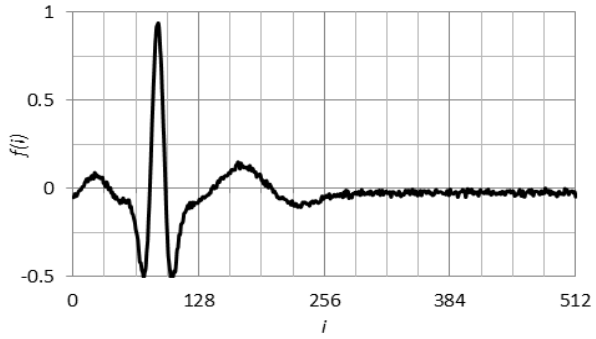

Fig.4. Modeled ECG signal $f(i)$ with superimposed Gaussian noise u_{eff}=10 mV.

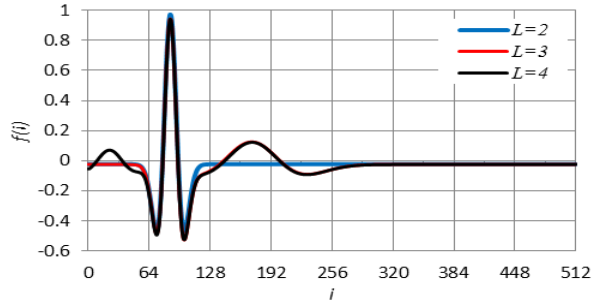

Fig.5. Recovered signal $\hat{f}(i)$ using L=2 to L=4 wavelets in $\mathbf{\Psi}$.

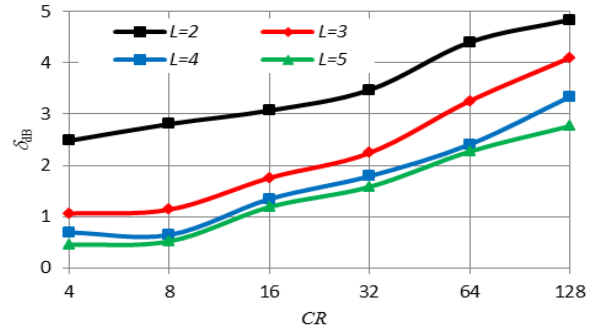

Fig.6. Standard deviation vs. compression ratio for L basis functions.

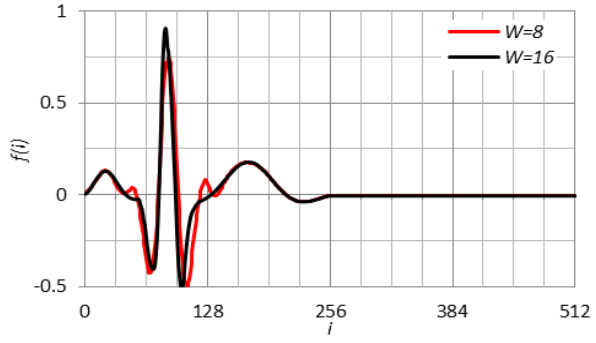

Fig.7. Recovered signal $f(i)$ from Fig.4. modeled by delayed Heaviside functions for different compression ratios. Compression of I=512 samples with averaging window of W=16 samples a) and W=8 samples b).

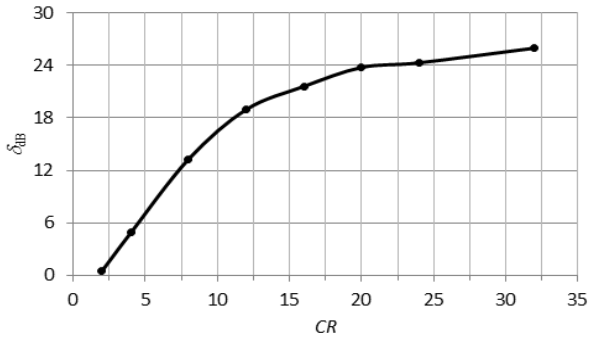

Fig.8. Accuracy of signal recovery using model (11) vs. compression ratio.

Comparison of the recovery efficiency using pseudoinverse procedure (8) was studied for the same ECG signal, Fig.4. The universal signal model by delayed Heaviside function (10) has been chosen. Recovered signals for various values of the compression ratio are shown in Fig.7.

In case of ECG signal, the sparsity s is higher when Heaviside model (3) is being used in comparison with the parametric model (2) with wavelets. As a result, the compression ratio for Heaviside model is lower. On the other hand, the exactness of the pseudoinverse procedure is the advantage of model (3).

Circuit implementation of the proposed AIC is feasible by the simple hardware block. The only analog processing block is ADC. Sensitivity and voltage range can be fixed by possible amplifier with gain control. Digital data from the ADC output are subsequently processed by digital blocks only. The PRBS is generated by algorithms for the determined polynomial length and initial value by the appropriate structure [18]. Averaging of data in the window of the length $W = I/M$ is the simplest LP filtering method. All numerical procedures for signal compression are easy to implement on the FPGA block or by the subroutines already available in the DSP unit.

Recovery of compressed data requires a mathematically more complex procedure. These are represented by the pseudoinverse calculus or an appropriate numerical optimization. Its selection from a wide range of optimization algorithms is conditioned by the guarantee of globally optimal solution for any class of problems which can be a problem for the nonlinear gradient method.

5. Conclusions

Compressed sensing is a method of signal processing reducing data stream in comparison with the requirement of the Nyquist theorem. Selection of the optimal set of basis functions allows highlighting the sparsity of the measured signals. Modulation by measurement matrix $\mathbf{\Phi}$ for signal decorrelation and successive low–pass filtering represents the basic architecture of the AIC. The hardware implementation with minimal amount of analog processing

blocks is the main advantage of the proposed AIC structure. Parameters of presented hardware structure are quite identical with possible implementation on the FPGA chip or other DSP unit.

Suitable set of basis functions depending on the input signal shape that has to be taken into account is the selection of the signal model $\mathbf{\Psi}$. Contrary to classical transformation compression the set of basis functions could not be orthogonal. Moreover, it may also consist of mutually different analytically described functions with defined position and shape in the synchronized time frame.

The signals with long time zero intervals and short pulse course are described optimally by linear model (3) together with unknown amplitudes $\hat{\mathbf{x}}$. The analytical calculation of vector $\hat{\mathbf{x}}$ is its main advantage, at the expense of lower compression ratio.

In contrast, the input signal recovery described by parametric signal model (2) leads to the numerical estimation of vectors $\hat{\mathbf{a}}, \hat{\mathbf{b}}, \hat{\mathbf{x}}$. When the observed process is unknown the optimal signal model could be adapted to the observed signal.

Performed simulations showed the significant trade-off between the computational complexity and achieved compression ratio for both signal models. Compressed sensing showed as well the positive impact of the proposed AIC on the noise suppression.

ACKNOWLEDGMENT

The work is a part of the project supported by the Science Grant Agency of the Slovak Republic (No. 1/0722/18).

REFERENCES

[1] Daponte, P., Vito, L., Rapuano, S., Tudosa, I. (2014). Challenges for aerospace measurement systems: Acquisition of wideband radio frequency using Analog-to-Information converters. In *IEEE Metrology for Aerospace (MetroAeroSpace)*. IEEE, 377-382.

[2] Pinheiro, E.C., Postolache, O.A., Girao, P.S. (2010). Implementation of compressed sensing in telecardiology sensor networks. *International Journal of Telemedicine and Applications*, 2010, 127639.

[3] Qaisar, S., Bilal, R.M., Iqbal, W., Naureen, M., Lee, S. (2013). Compressive sensing: From theory to applications, a survey. *Journal of Communications and Networks*, 15 (5), 443-456.

[4] Boche, H., Calderbank, R., Kuttyniok, G., Vybíral, J. (2015). *Compressed Sensing and its Applications*. Springer.

[5] Slavik, Z., Ihle, M. (2014). Compressive sensing hardware for analog to information converters. In *8th Karlsruhe Workshop on Software Radios*, 136-144.

[6] Candés, E.J., Becker, S. (2013). Compressive sensing: Principles and hardware implementations. In *Proceedings of the ESSCIRC*. IEEE, 22-24.

[7] Faktor, T., Michaeli, T., Eldar, Y.C. (2010). Nonlinear and nonideal sampling revisited. *IEEE Signal Processing Letters*, 17 (2), 205-208.

[8] Xu, D., Tongret, R., Zheng, Y.F., Ewing, R.L. (2010). Wavelet modulated pulse for compressive sensing in sar. In *Proceedings of the IEEE 2010 National Aerospace and Electronics Conference (NAECON)*. IEEE, 197-202.

[9] Maleh, R., Fudge, R., Member, G.L., Boyle, F.A., Pace, P.E. (2012). Analog-to-information and the Nyquist folding receiver. *IEEE Journal on Emerging and Selected Topics in Circuits and Systems*, 2 (3), 564 -577.

[10] Yu, Z., Hoyos, S. (2009). Digitally assisted analog compressive sensing. In *IEEE Dallas Circuits and Systems Workshop (DCAS)*. IEEE, 1-4.

[11] Barkam, E., Biham, E., Keller, N. (2008). Instant ciphertext-only cryptanalysis of GSM encrypted communication. *Journal of Cryptology*, 21 (3), 392-429.

[12] Liu, W., Huang, Z., Wang, X., Sun, W.C. (2017). Design of a single channel modulated wideband converter for wideband spectrum sensing: Theory, architecture and hardware implementation. *Sensors*, 17 (5), 1035.

[13] Davenport, M.A., Duarte, M.F., Eldar, Y.C., Kutyniok, G. (2012). Introduction to compressed sensing. In *Compressed Sensing: Theory and Application*. Cambridge University Press, 1-64.

[14] Press, W., Teukolsky, S., Vetterling, W., Flannery, B. (2007). *Numerical Recipes: The Art of Scientific Computing, Third Edition*. Cambridge University Press, 386.

[15] Andráš, I., Dolinský, P., Michaeli, L., Šaliga, J., (2018). Sparse signal acquisition via compressed sensing and principal component analysis. *Measurement Science Review*, 18 (5), 175-182.

[16] Duarte, M.F., Eldar, Y.C. (2011). Structured compressed sensing: From theory to applications. *IEEE Transactions on Signal Processing*, 59 (9), 4053-4085.

[17] Tropp, J.A., Laska, J.N., Duarte, M.F., Romberg, J.K., Baraniuk, R.G. (2010). Beyond Nyquist: Efficient sampling of sparse bandlimited signals. *IEEE Transactions on Information Theory*, 56 (1), 520-544.

[18] Storn, R.M., Lampinen, J.A. (2005). *Differential Evolution: A Practical Approach to Global Optimization*. Springer.

[19] Michaeli, L., Šaliga, J., Godla, M., Lipták, J., Kollár, I. (2014). Measurement of distorted exponential signal components using maximum likelihood estimation. *Measurement*, 58, 503-510.

[20] Dolinsky, P., Andraš, I., Michaeli, L., Grimaldi, D. (2018). Model for generating simple synthetic ECG signals. *Acta Electrotechnica et Informatica*, 18 (3), 3-8.

[21] Li, S., Xu, L.D., Wang, X. (2013). A continuous biomedical signal acquisition system based on compressed sensing in body sensor networks. *IEEE Transactions on Industrial Informatics*, 9 (3), 1764-1771.

[22] ElProCus. *PIR sensor – basics & applications*. https://www.elprocus.com/pir-sensor-basics-applications/

[23] PhysioNet. *PhysioBank databases*. https://physionet.org/physiobank/database/

[24] Silvan Chip Electronics Tech. Co., Ltd. *BISS0001 PIR controller.* http://www.adrirobot.it/datasheet/speciali/pdf/BISS0001.pdf.

[25] Candes, E., Romberg, J. (2005). Practical signal recovery from random projections. In *Wavelet Applications in Signal and Image Processing XI. Proceedings of the SPIE 5914.*

Received May 25, 2018
Accepted January 24, 2019